Domenech Carbo, MT.; De Sousa Ramos Félix Silva, M.; Aura-Castro, E.; Fuster López, L.; Kröner, SU.; Martínez Bazán, ML.; Mas Barberà, X.... (2011). Study of behaviour on simulated daylight ageing of artists' acrylic and poly(vinyl acetate) paint films. Analytical and Bioanalytical Chemistry. 399(9):2921-2937. doi:10.1007/s00216-010-4294-3.

Anal Bioanal Chem
DOI 10.1007/s00216-010-4294-3

ORIGINAL PAPER

Study of behaviour on simulated daylight ageing of artists' acrylic and poly(vinyl acetate) paint films

María Teresa Doménech-Carbó · Miguel F. Silva · Elvira Aura-Castro · Laura Fuster-López · Stephan Kröner · María Luisa Martínez-Bazán · Xavier Más-Barberá · Marion F. Mecklenburg · Laura Osete-Cortina · Antonio Doménech · José Vicente Gimeno-Adelantado · Dolores Julia Yusá-Marco

Received: 28 July 2010 / Revised: 28 September 2010 / Accepted: 4 October 2010

Abstract This work proposes a multi-method approach that combines advanced microscopy (SEM/EDX, AFM) and spectroscopy (UV-vis and FTIR) techniques. This approach not only characterises the behaviour of the additives of two commercial poly(vinyl acetate) (PVAc) and acrylic emulsion paints but also simultaneously characterises the changes in chemical composition and morphology observed in the paint films as a result of ageing due to the paints being exposed to an intense source of simulated daylight. In parallel, a series of mechanical tests were performed that correlate the chemical changes in composition and the changes observed in the films' mechanical properties. This work was a comparative study between both types of acrylic and PVAc paints. The results obtained are of great interest for the modern paints conservation field as they provide valuable information on the mid- and long-term behaviours of these synthetic paints.

Keywords Surfactant · Acrylic artists' paint · PVAc paint · FTIR spectroscopy · AFM · Tensile tests

Published in the special issue *Analytical Chemistry for Cultural Heritage* with Guest Editors Rocco Mazzeo, Silvia Prati and Aldo Roda

M. T. Doménech-Carbó (✉) · M. F. Silva · E. Aura-Castro · L. Fuster-López · S. Kröner · M. L. Martínez-Bazán · X. Más-Barberá · L. Osete-Cortina · D. J. Yusá-Marco
Instituto de Restauración del Patrimonio,
Universidad Politécnica de Valencia,
Camino de Vera s/n,
46022 Valencia, Spain
e-mail: tdomenec@crbc.upv.es

M. F. Mecklenburg
Museum Conservation Institute, Smithsonian Institution,
4210 Silver Hill Road,
Suitland, MD 20746-2863, USA

A. Doménech · J. V. Gimeno-Adelantado
Dpt. Química Analítica. Facultad de Química,
Universidad de Valencia,
Avda. Doctor Moliner s/n,
46100 Burjassot, Spain

Introduction

The characterisation of artists' materials and the identification of the deterioration products and mechanisms affecting them are critical to fully understand the reasons for their corrosion or deterioration and to determine the appropriate treatment and storage environment. In the twentieth century, synthetic polymers significantly replaced the application of traditional binding media used in paintings because of their excellent physical properties and special applications. Their wide variety of formulations mean that these materials are most useful as not only binding media but also as varnishes, consolidants and adhesives for painting or filling the missing parts used in restoration works with stone materials and archaeological objects, among others.

Acrylic and poly(vinyl acetate) (PVAc) resins started to be employed as paint media by artists thanks to some of their properties such as reduced drying times and low yellowing if compared with media based on drying oils. These synthetic media are usually provided in the form of an emulsion of methyl methacrylate–ethyl acrylate and butyl acrylate–methylmethacrylate co-polymers for acrylic media and as vinyl acetate co-polymerised with other softer monomers such as *n*-butyl acrylate, 2-ethtylhexyl acrylate and, most frequently, highly branched C_9 and C_{10} vinyl esters. The acrylic and PVAc emulsions used as binding media for artists' paints are produced by an emulsion

polymerisation technique [1]. Commercial artists' emulsion paints include a number of compounds, as well as synthetic polymers and pigments, that improve the physical and chemical properties of the resulting product [1, 2]. Among the most frequent additives of artists' emulsion paints, we find coalescing agents, defoamers, freeze–thaw agents, pH buffers, preservatives and biocides, protective colloids, sequestering agents, surfactants, thickeners and wetting and dispersing agents.

A number of studies can be found in the specialised literature that identify the additives present in the commercial brands of PVAc [3] and acrylic paints [4, 5] habitually used by artists, particularly those compounds used as surfactants. Poly(ethylene glycol) (PEG)-based additives, polypropylene glycol (PPG) and a block copolymer of polyethylene glycol/polypropylene glycol (PEG/PPG) with different molar mass averages have been recently reported as frequently used surfactants in acrylic emulsion paints [4]. Nonylphenyl or octylphenyl hydrophobic end groups and hydroxide and/or sulphate end group hydrophilic end groups are those most commonly found in PEG-based additives [4].

Non-ionic polyethylene oxide (PEO) or polyethoxylate-based compounds have been identified as surfactants in PVAc paints, together with cellulose ether-type compounds used as thickeners. The presence of phosphate-type compounds (flame retardant) and methenamine (preservative) as well as styrene and methacrylic acid has also been reported for PVAc paints [3].

In the last few decades, deterioration of synthetic polymers due to the weathering effect of light, exposure to air containing various atmospheric pollutant gases and changes in temperature or humidity has been a subject of interest for a number of researchers working in the conservation science field [6–12].

Elimination, depolymerisation and random scission are the main energy-induced processes (which do not require external molecules) that commonly affect synthetic polymers. These processes can take place throughout thermal or photolytic mechanisms. In addition to these, thermal and photo-oxidative reactions can occur when the polymer is found in the presence of air. These reactions generally follow a free radical chain reaction sequence. Such processes mainly result in the formation of oxygenated functional groups such as carbonyl, alcohol, ether or hydroperoxide in the polymer backbone. The chain scission and/or coupling of macroradicals, cross-linking between chains and emission of small molecules (CO, CO_2, H_2O, H_2O_2, carboxylic acids and ketones), can also take place in aerial environments. Another important deterioration path is owed to water attacking the hydrolysis-sensitive groups present in the polymer. If target bonds are part of the polymer backbone chain, then depolymerisation is the preferential deterioration route. When functional groups are attached to the side of the backbone chain, various small molecules are released. Finally, a number of atmospheric gases, such as ozone and oxides of sulphur and nitrogen, can also induce deterioration mechanisms.

As mentioned above, a number of deterioration processes which do not require external molecules are prompted by the exposure of a polymer to an intense light source. In addition to these processes, oxidative deterioration processes can be greatly accelerated by irradiating the polymer with light, and, for this reason, the effect of light exposure on acrylic and PVAc polymers, used mainly as the binding media of modern paints, has been increasingly surveyed.

Ageing tests performed on acrylic polymers used as protective coatings of monuments and as artists' media have revealed that these polymers can undergo chain-breaking, photo-oxidation and cross-linking, to different extents, when irradiated and depending on the light source (natural UV-A, UV-B or artificially simulated sunlight) [7]. Chain scission has been reported to be the preferential deterioration route of acrylic coatings under ultraviolet irradiation [11]. In a comparative study conducted between different types of acrylic polymers, Chiantore et al. [8] found that acrylate-type polymers are more reactive towards oxidation processes than methacrylate ones. A number of authors have reported that acrylic polymer stability is strongly influenced by the length of the alkyl side chain [13]. Acrylic polymers containing longer alkyl side-chain groups, such as *n*-butyl and *iso*-butyl, are more prone to cross-linking and, to a lesser extent, to chain-breaking. Oxidation in these compounds is favoured by the presence of relatively labile hydrogen atoms [9]. In contrast, chain scission prevails in those acrylic polymers containing shorter alkyl side-chain groups, such as methyl or ethyl, accompanied by macromolecular coupling reactions so that the molecular characteristics of the acrylic polymer are maintained during ageing. Photo-oxidative reactions, resulting in the formation of γ-lactones and cross-linking, have also been reported as deterioration pathways that take place, to a lesser extent, in this type of polymers [8].

More recent studies performed on acrylic emulsion paints, which have naturally and artificially aged with simulated sunlight, indicate that these types of polymers are highly stable for photo-oxidation and that they display a certain tendency to chain-breaking rather than to cross-linking [9, 10].

PVAc polymers subjected to UV light exposure undergo chain scission, cross-linking and the release of volatile compounds, mainly acetic acid and, to a lesser extent, carbon monoxide, carbon dioxide and methane [14]. In contrast, recent studies performed on PVAc paints irradiated at $\lambda \geq 300$ nm have revealed that no side-group scission

takes place and that the main chain scission is the principal photodegradation mechanism [15].

The effect of pigments acting as catalysts has also been reported. In particular, the rate and induction time of photo-oxidation reactions have been seen to be notably affected by cobalt blue in acrylic paint emulsions [10].

The behaviour of the additives also present in modern paint formulations during drying and ageing processes not only influences chemical and mechanical properties but also the visual appearance of the paint film.

During the drying process of acrylic paint films, the surfactant slowly segregates to the paint film surface to form microscopic crystalline inclusions [16], as well as characteristic aggregates [2, 17, 18]. These phenomena have been reported to be the result of the uncontrolled migration of the additive to the paint–air interface [2]. Loss of the non-ionic polyethoxylated-type surfactant during artificially simulated sunlight ageing has also been reported [6]. In addition, this class of surfactant undergoes noticeable oxidative chain scission during artificially simulated sunlight ageing [10].

Loss of diethyl and dibutyl phthalates, present in a number of commercial PVAc artists' media used as an external plasticiser, has also been reported after artificially ageing these specimens by thermal ageing and irradiation with UV light [19].

This work proposes a multi-method approach that combines advanced microscopy (scanning electron microscopy (SEM)/energy-dispersive X-ray (EDX), atomic force microscopy (AFM)) and spectroscopy (UV-vis and FTIR) techniques. This approach was followed to not only characterise the behaviour of the additives of two commercial PVAc and acrylic emulsion paints but to also simultaneously characterise the changes in the chemical composition and morphology observed in the paint films as a result of ageing due to the paints being exposed to an intense source of simulated daylight. In parallel, a series of mechanical tests were performed in an attempt to correlate the chemical changes in composition and the changes in the film's mechanical properties. This work was a comparative study between both types of acrylic and PVAc paints. The results obtained are of great interest in the modern paints conservation field as they provide valuable information on the mid- and long-term behaviours of these synthetic paints.

Experimental

Reference materials and commercial artists' emulsion paints studied

Polyethylene glycol (PEG 1500) was supplied by Kremer Pigmente.

Four different acrylic emulsion paints were selected for this study: burnt umber, phthalocyanine blue, naphthol red and zinc oxide Liquitex® heavy body. Liquitex® paints are prepared with a butyl acrylate–methyl methacrylate-based medium.

In parallel, four PVAc emulsion paints were studied: Oriental red, Green armour, Senegal yellow and Burnt Sienna Flashe®.

Instrumentation

Light microscopy Microsamples were examined under a Leica DMR microscope using reflected light at the ×25 to ×400 magnification.

Scanning electron microscopy–energy-dispersive X-ray microanalysis Surfaces and cross sections of the film specimens were monitored using a Jeol JSM 6300 scanning electron microscope operating with a Link-Oxford-Isis X-ray microanalysis system. The analytical conditions were 10-kV accelerating voltage and 2×10^{-9}A beam current. Samples were gold-coated to eliminate charging effects.

Atomic force microscopy To evaluate the films' surfaces, a Multimode AFM (Digital Instruments VEECO Methodology Group, USA) with a NanoScope IIIa controller was used, equipped with a J-type scanner (max. scan size of 150×150×6 mm). The topography of samples was studied in the tapping mode. The cantilever (Olympus Tapping Mode etched silicon probes, Veeco Methodology group) has a spring constant of ~42 N/m and a radius of 5–10 nm to ensure good imaging resolution and nanometre-scale indents. Images were obtained using probe excitation frequencies of 300 kHz. All the images were captured at a scan rate of 0.5–1 Hz. A set point to the free amplitude ratio (Rsp) of 0.75, corresponding to a 25% attenuation of the amplitude of vibration, was used for all the images.

FTIR spectroscopy The infrared (IR) spectra in the attenuated total reflectance (ATR) mode of the film specimens were obtained using a Vertex 70 Fourier transform infrared spectrometer with an fast-recovery deuterated triglycine sulphate, temperature-stabilised coated detector and an MKII Golden Gate ATR accessory. A total of 32 scans were collected at a resolution of 4 cm^{-1}, and the spectra were processed using the OPUS/IR software.

Spectrophotometry UV-vis The spectra in the UV and visible regions were obtained using a Perkin Elmer Lambda 1,050 recording double-beam spectrophotometer. Reflectance measurements were carried out in the range from 200 to 850 cm^{-1}.

The L^*, a^*, b^*, C^*, h^* and E^* coordinates were obtained with a Minolta CM-503i spectrophotometer using a Xe-arc lamp and a Si photodiode detector. The instrument was calibrated with standard white (coordinates Y 95.8; x 0.3167; y 0.3344).

Tensile testing The equipment consisted of a rectangular methacrylate box containing several tensile testers. This box acts as a climatic chamber where relative humidity (RH) and temperature (T) can be kept constant. Test specimens were supported in tensile clamps, and additional fringed areas were retained at the edges. Average sample measurements were 5 mm (width) × 0.12 mm (thickness) and 20-mm length. Specimens were mounted in testing gauges and conditioned in the chamber for 48 h at 50± 0.5% RH and 23±0.5 °C prior to testing. Model paint specimens were measured under the same environmental conditions. Then, 0.05 strain increments were applied progressively at 30-s intervals. Three identical specimens were tested for each model paint film. An overlap of three to five curves in all the tests demonstrated the repeatability of the testing procedure.

Preparation of test specimens

Test specimens were obtained as thin paint films by casting the previously mentioned Liquitex® and Flashe® paint colours over Mylar® sheets. Paint films were dried under the environmental conditions for 1 year. Afterwards, the resulting films, which had acquired an average thickness of 0.15 mm, were subjected to an accelerated light exposure test by means of irradiation with simulated daylight from a xenon arc source, as described in the following section.

Simulated daylight ageing

Light exposure tests were carried out in an ATLAS Ci4000 Weather-O-metre with Xenon Arc Lamp Type S-filter radiation. Test conditions were 1.1 W/m^2 in the visible range at 420 nm (115,000 lx) and 56 W/m^2 at 300–400 nm. The average temperature was 26 °C for the 400-h ageing test and 27 °C for the 800-h ageing test. Relative humidity (%RH) was 35–40%. The black panel temperature was 42 °C, while the black standard temperature was 52 °C.

As previously mentioned, the behaviour of the polymers used as artists' media in modern paints was notably influenced by the characteristics of radiation to which these materials were exposed. For this reason, a xenon-arc-type radiation source, which closely matches the sunlight spectrum, was selected to perform a photo-ageing test that closely reproduces the natural ageing conditions to which the studied modern paints are subjected in museums and collections. The xenon arc lamp selected provides light in the visible and UV regions with a similar electromagnetic spectrum to that of natural daylight. The equipment was equipped with a filtering system that significantly reduces the intensity of the wavelengths emitted below 300 nm so that irradiated light is comparable to sunlight, except for its notably higher intensity.

On the other hand, temperature and relative humidity were maintained at low values (27 °C, 35–40% RH) in an attempt to the minimise the reactions induced thermally and by hydrolysis.

The accelerated weathering experiment subjected the model paint specimens to radiation exposure in two 400-h steps. In this way, the irradiation doses corresponding to the 400- and 800-h exposure times could be checked. These values were chosen in accordance with the intensity values of the light emitted by the xenon arc lamp used and according to Feller's stability classification of materials [20]. Thus, the two light exposure doses to which specimens were subjected can be equated to the exposure doses on display in a museum of a member material of Feller's stability "class B" (for the 400-h exposure time) and of a member material of Feller's stability "class A" (for the 800-h exposure time). According to Feller's model, the materials included in class B satisfactorily maintain their properties between 20 and 100 years, whereas those materials classified as class A adequately maintain their properties up to 100 years.

For establishing the light exposure time values in the accelerating ageing test, the corresponding exposure doses were equated to the equivalent values of doses in museum environments, as previously reported in the literature, by following Bunsen and Roscoe's classical model [21] for the reciprocity principle. Thus, 104 and 208 "museum years" values were obtained as the equivalent to the artificial ageing doses reached after 400 and 800 h, respectively, based on the exposure dose values in museums provided by Whitmore and Colaluca [7]. Similarly, 77 and 153 "museum years" values were obtained for 400 and 800 h, respectively, based on the exposure dose values in museums according to Learner et al. [6].

A second series of calculations were made to select the experimental exposure times using the model of Schwarzschild [22] for the reciprocity principle, which can be mathematically expressed as:

$$I \cdot \mathrm{x} \cdot t^p = k$$

where I is the intensity of the light source, and t is the exposure time; the p, power, is a constant value, and k is also a constant value. In this case, 103 and 214 "museum years" values were obtained for the exposure times of 400 and 800 h, respectively, for the p power values in the 1–1.05 range using the exposure dose values in museums according to Learner et al. [6].

Q1

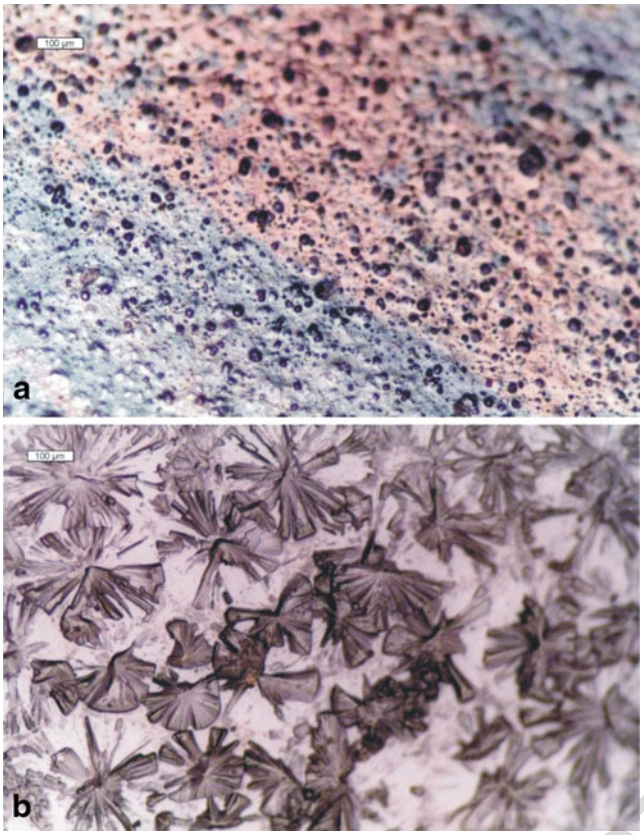

Fig. 1 **a** Alteration in the visual appearance of the phthalocyanine blue Liquitex® film specimen due to the migration of the additive. **b** Detail of the thin layer of the additive compounds migrating from the paint core to the surface, which has acquired a reddish haze

Results and discussion

Micromorphology and chemical composition

Unaged model paint films

No significant migration of additives from the bulk to the Flashe® films surface was observed in the studied model paints series after examining specimens' surfaces by light microscopy. In contrast, some morphological changes were observed in the Liquitex® series. Thus, phthalocyanine blue paint displayed the formation of a translucent thin layer on some areas of films' surfaces, which was attributed to the surfactant migrating from the bulk to the film surface. This layer gave the film a reddish appearance (Fig. 1a). The spots surrounding the large and deep pits eventually formed in the burnt Sienna paint film. The zinc oxide paint film showed a more noticeable alteration, consisting of characteristic microcrystalline aggregates in a stellate habit that spread on the surface (Fig. 1b). Interestingly, in this case, the morphological changes on the film surface were seen to be in contact with the Mylar film used as a support. This behaviour has been reported in methyl methacrylate–ethyl acrylate–methacrylic acid terpolymer where the latex particle surface was enriched in the highly hydrophilic methacrylic acid groups [23].

Examination of the paint film specimens' cross sections provided complementary information to that obtained from the surfaces. The binding medium in the Flashe® paints was hardly recognised in the cross sections, where pigment grains were abundant and closely packed. In contrast, "pockets" or agglomerates of the surfactant and organic additives that remained trapped in the bulk film were observed in the studied Liquitex® paint series (Fig. 2).

Atomic force micrographs were taken from the surfaces of the unaged paint samples and confirmed the results previously obtained by light microscopy (LM) and SEM. Liquitex® paints generally exhibited a smoother surface than Flashe® paints in the (2×2)- and (5×5)-μm-scale ranges studied. Thus, an average value of Δz of 2,000 (Δz is defined as the maximum peak-to-valley distance measured in the paint surface area examined by AFM) was found for the studied Flashe® paint series' replicates on the air–film surface (see Fig. 3a). This value is associated with the height of the pigment grains protruding on the binding medium after this had dried. Liquitex® HB paints exhibited a lower Δz value of 1,000 on the air–film surface (see Fig. 3b), although the zinc oxide paint film obtained a higher value of 2,000 nm. The superficial density of the pigment grains was also higher in Flashe® paints than in Liquitex® ones. These results suggest that the studied commercial PVAc brand presented a greater pigment content than the acrylic Liquitex® brand.

The reflectance spectra on the surface were obtained from the areas of the Liquitex® phthalocyanine blue and zinc oxide paint films where additives were seen to migrate. The features appearing in the visible region correspond to

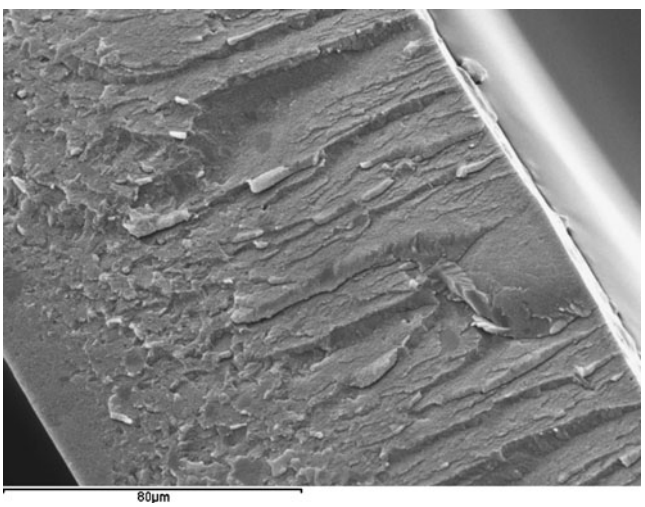

Fig. 2 Secondary electron microphotograph of the cross section of Liquitex® phthalocyanine blue paint film showing agglomerates of the additives trapped within the bulk film

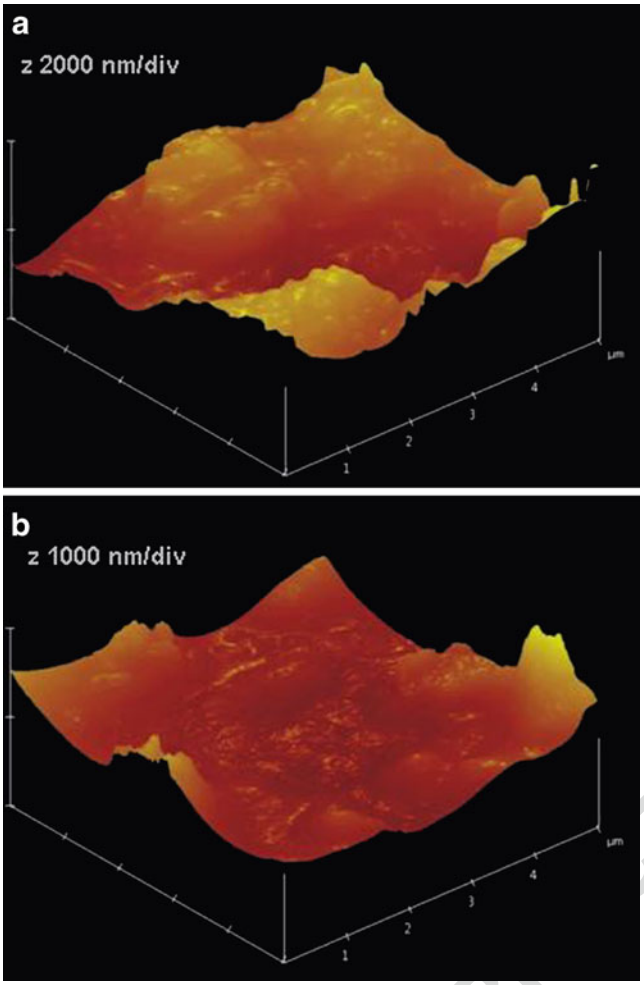

Fig. 3 Atomic force micrographs showing the air–film surface of: **a** unaged Senegal yellow Flashe® paint film; **b** unaged burnt umber Liquitex® paint film

pigment, whereas the UV region provides interesting data on the additives (mainly the surfactants used as stabilisers) that migrated to the paint film surfaces. Thus, zinc oxide showed a high reflectance value (>80%) in the overall visible region. The spectrum obtained in the UV region from this paint film surface, where microcrystalline aggregates were deposited, exhibited weak bands with maxima at 273 and 227 nm (Fig. 4a). Phthalocyanine blue presented a reflectance band with a maximum at 429 nm (the blue range) and a weak band with a maximum at 566 nm (the yellow region). At 700 nm, a broad reflectance band with two maxima at 805 and 779 nm was observed (Fig. 5a), and this band could be associated with the additive that migrated to the surface (see Fig. 1a), which selectively reflected light in the red range. The reflectance spectrum in the UV region exhibited weak reflectance bands with maxima at 275 and 228 nm, which were ascribed to the surfactant deposited on the film surface (Fig. 5b) [16].

The chemical composition changes were evaluated by comparing the IR absorption spectra obtained before and after simulated daylight ageing. The measurements taken in the total attenuated reflectance mode provide the average film composition on its outer layer (depth in the 0.22–0.66 μm range) [24].

Table 1 summarises the main IR absorption bands of analytical interest identified in the studied Liquitex® model paint films series. The IR spectra of the unaged paint films were dominated by the acrylic binding medium's IR absorption bands. In particular, the IR bands appearing at 2,955 and 2,932 cm^{-1} were ascribed to the $–CH_3$ and $–CH_2$ antisymmetric stretching vibration of the acrylic polymer's hydrocarbon skeleton; the IR band at 1,730 cm^{-1} was associated with the stretching vibration carbonyl groups in the acrylate and methacrylate groups, while the IR band at 1,146 cm^{-1} was associated with the stretching vibration of the –C–C(=O)–O bonds in the ester groups. Weak and sharp IR absorption bands were observed, which were ascribed to the hydroxylic groups (3,400–3,100 $cm^{-}1$) and aromatic rings (1,700–1,600 cm^{-1} and 900–600 cm^{-1}) present in the naphthol red and Phthalo blue pigments, be it at a lesser extent. The intense IR bands at 2,894–78, 1,113 cm^{-1} ascribed to a non-ionic surfactant of the PEO type which eventually migrated to the film surface, were also observed in the unaged zinc oxide paint film. It is interesting to note that the zinc oxide and burnt umber paint films exhibited a broad, weak band at 1,563 cm^{-1}, which was tentatively assigned to the COO-asymmetric stretching vibrations relating with the metal–carboxylate complexes. The appearance of this band in these paint films, including those pigments of an inorganic nature, suggests that the manufacturer could, to some extent, include a poly(acrylic) type thickener or an anionic surfactant together with this non-ionic PEO type in an attempt to improve the degree of electrostatic stabilisation of the inorganic pigment in emulsion [25].

The main IR absorption bands of analytical interest identified in the studied Flashe® model paint films series are summarised in Table 2. Flashe® paint films exhibited IR absorption spectra dominated by the IR bands of calcium carbonate at 1,410, 871 and 712 cm^{-1}. This pigment was included by the manufacturer as an extender in the commercial formulation of paints. Intense IR bands were also observed in the PVAc medium at 2,961, 2,926, 2,873, 1,736, 1,232, 1,372 and 1,086 cm^{-1}. A weak IR absorption band was identified at 1,046 cm^{-1}, which has been ascribed to a non-ionic surfactant of the PEO type.

Aged model paint films

Secondary electron images and atomic force micrographs from the surface of simulated daylight-aged paint films

Q1

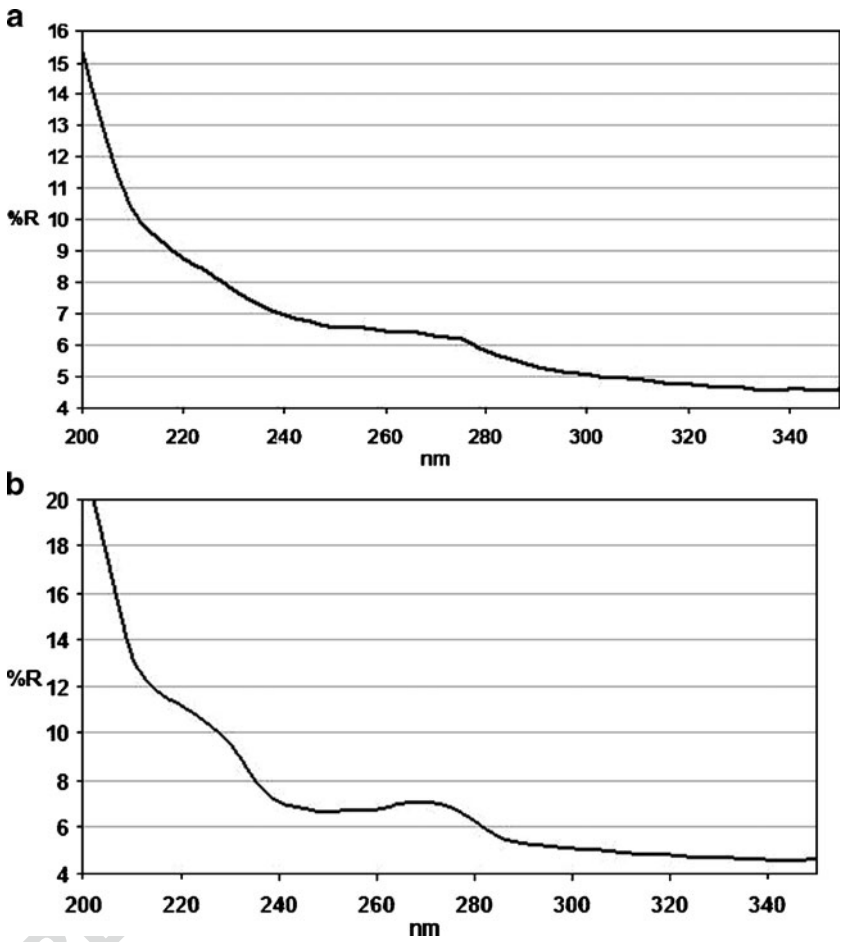

Fig. 4 Reflectance spectrum of the zinc oxide Liquitex® paint film in the UV region of **a** unaged paint film; **b** 800-h simulated-daylight-aged paint film

show that irradiated paints generally exhibited a smoother surface. The Δz value dropped from 2,000 to 1,000 nm in the Senegal yellow films and from 500 to 300 nm in the other three Flashe® paint films for air–film surfaces. These morphological changes in film surface correlate to the changes noted in the polymer structure, which are mainly associated with photodegradation (vide infra). Similarly, a decrease in the Δz values in the 1,000–800 nm range was observed on the air–film surfaces of the studied Liquitex® paint films (Fig. 6a), apart from the zinc oxide paint film for which no significant changes were observed. These results may be associated with the smoothing effect due to the structural changes taking place in the polymer, particularly cross-linking [26] and also to the exudation of the material from within the film, most probably the PEO-type chained surfactant used as a stabiliser [27]. Further gradual coalescence of the film [28, 29], which should take place to a greater extent on air–film surfaces as the result of irradiation with simulated daylight, may also contribute to this smoothing effect on the paint surface. This hypothesis is supported by the AFM micrographs obtained on the film–substrate surface of some of the studied paint films stored under the environmental conditions for 1 year. In this case, a typical honeycomb-type latex substructure was recognised (see Fig. 6b). This morphology evidences that the coalescence phase in the core of these acrylic paints' film was still incomplete after 1 year.

The results obtained by microscopy techniques were confirmed by colorimetric measurements. Table 3 summarises the shift of the values of the L^*, a^* and b^* coordinates, as well as the chrome (C^*), hue (h^*) and total colour (E^*) obtained after the simulated daylight ageing of the studied model paint films. Figure 7 depicts the behaviour of the paints as a result of accelerated ageing, where arrows represent the changes in the position of each paint in the CIELAB diagram after simulated sunlight ageing. Noticeable changes in the values of the a^* and b^* coordinates and, consequently, in the C^* and h^* values, were observed in both the studied model paints series, except zinc oxide Liquitex® whose initial values scarcely modified. These changes were mainly associated with the fading effect of light exposure on the pigments, irrespective of their commercial brand. The general tendency observed in the model paints was a lowered chrome value (given by the expression $C^* = \left(a^{*2} + b^{*2}\right)^{1/2}$) to a greater or lesser

JnlID 216_ArtID 4294_Proof# 1 - 12/10/2010

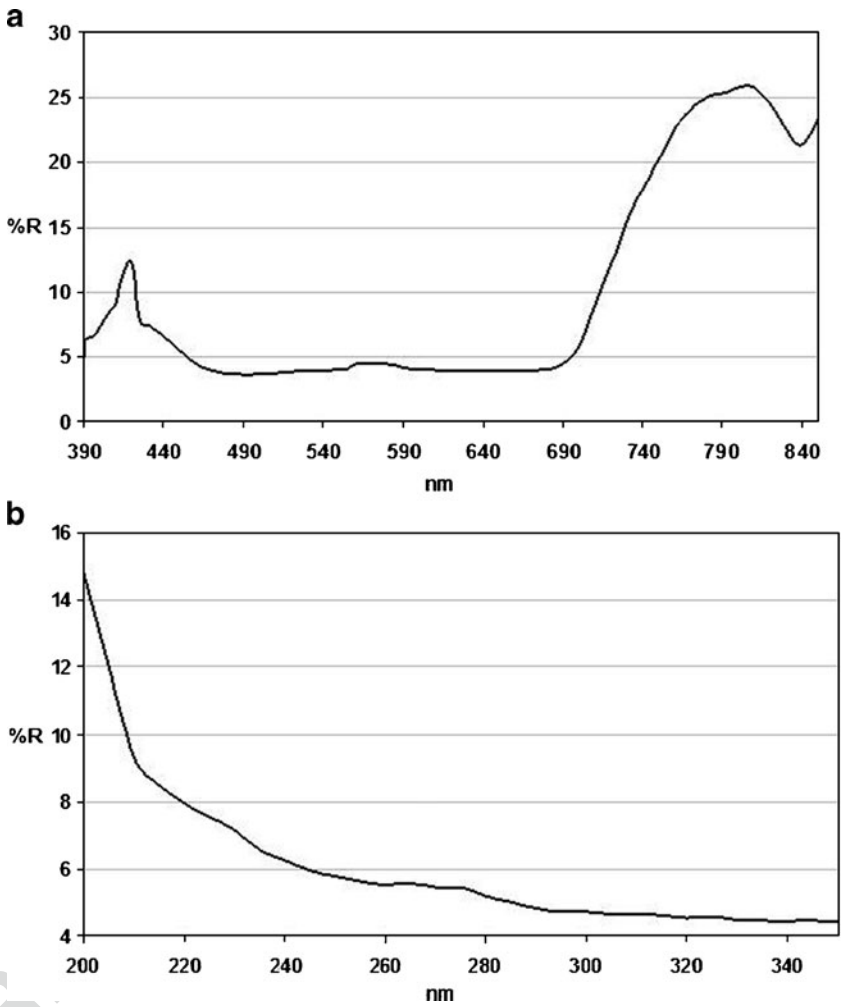

Fig. 5 Reflectance spectrum of the unaged Liquitex® phthalocyanine blue paint film in the **a** visible region and **b** UV region

extent depending on each pigment's sensitivity to light. Thus, the a^* and b^* values of the two red paints studied (Oriental red Flashe® and Naphthol red Liquitex®) lowered to the extent that they were finally placed closer to the origin of the coordinates in the CIELAB space. An analogous behaviour was observed for burnt Sienna Flashe® and for burnt umber Liquitex®. In a series of former experiments, an organic pigment was identified in the burnt Sienna Flashe® paint, which was probably added by the manufacturer to improve the paint's colour [30]. The greater shift of the a^* and b^* coordinates exhibited by this latter paint, if compared with those from the remaining paints containing pigments of an inorganic nature, may be due to this organic pigment being more sensitive to light exposure. Finally, Senegal yellow Flashe®, Green Armour Flashe® and Phthalo blue Liquitex® exhibited Δa^* and Δb^* values (resulting in a ΔC^* value), which also justifies the same tendency to undergo fading as that exhibited by the rest of the studied paints. The Δh^* values obtained in the series of studied paints were both moderate in magnitude and negative, except those from Green Armour and burnt Sienna Flashe® which exhibited a positive h^* shift. These results suggest that colour change was non-significant during the ageing process and, in particular, that the yellowing of the paints did not extensively take place under the experimental ageing conditions.

In general, the L^* value of the Flashe® films notably increased after the 800-h simulated daylight ageing, except for Senegal yellow whose L^* value slightly increased. Similarly, the L^* value of the Liquitex® series noticeably increased after simulated daylight exposure, apart from zinc white whose L^* value only slightly increased. By assuming that the smoothing effect of the films' surfaces favours the films' enhanced brightness, the results obtained are in good agreement with those obtained by AFM, which showed that the surfaces of paint films generally became smoother after exposure to simulated daylight.

The UV spectrum obtained on the surfaces of Liquitex® paint films also confirms the results obtained by SEM, AFM and Fourier transform IR (FTIR) spectroscopy (vide infra); thus, a noticeable increase in the absorption bands ascribed to the surfactant was observed in the UV region of the spectra of the films irradiated at 400 and 800 h with simulated daylight (Fig. 4b).

JrnlID 216_ArtID 4294_Proof# 1 - 12/10/2010

Q1

t1.1 **Table 1** The IR absorption bands of analytical interest identified in the studied Liquitex® HB model paint film series before and after the 800-h simulated daylight exposure

t1.2	IR absorption band (cm^{-1})	Functional group assignment	Compound assignment
t1.3	3,400	–OH associated stretching vibration	Water of hydration, diversified hydroxylic structures
t1.4	3,416, 3,393, 3,185	–OH stretching vibration	Naphthol red
t1.5	2,955, 2,932	$–CH_3$ and $–CH_2$ antisymmetric stretching vibration	Acrylic medium, polyethoxylated non-ionic surfactant
t1.6	2,884	$–CH_3$ symmetric stretching vibrations	Polyethoxylated non-ionic surfactant, acrylic medium
t1.7	1,730, 1,720	–C=O stretching vibration associated to acrylate and methacrylate groups and free acid groups	Acrylic medium
t1.8	1,681	–C=C– stretching vibrations, aromatic ring	Naphthol red, phthalo blue
t1.9	1,658	–C=C– stretching vibrations, aromatic ring	Naphthol red, phthalo blue
t1.10	1,643	–OH bending vibration	Water of hydration associated to clay (Burnt Umber)
t1.11	1,620	–OH bending vibration	Burnt umber, zinc oxide
t1.12	1,609	–C=C– stretching vibrations, aromatic ring	Naphthol red, phthalo blue
t1.13	1,563	COO– asymmetric stretching vibrations associated to carboxylate groups	Metal–carboxylate
t1.14	1,466	$–CH_2–$ symmetric bending vibration	Polyethoxylated non-ionic surfactant
t1.15	1,452	$–CH_3$ asymmetric bending vibration	Acrylic medium
t1.16	1,387	$–CH_3$ symmetric bending vibration	Acrylic medium
t1.17	1,359	Bending vibration $–CH_2$ group	Polyethoxylated non-ionic surfactant
t1.18	1,339	Bending vibration $–CH_2$ group	Polyethoxylated non-ionic surfactant
t1.19	1,279	–C–O stretching mode of alcohol groups	Polyethoxylated non-ionic surfactant
t1.20	1,240	Stretching mode of –C–C(=O)–O–C– of ester groups	Acrylic medium
t1.21	1,160	Stretching vibration of –C(=O)–O–C of butyl acrylate group	Acrylic medium
t1.22	1,146	Stretching vibration –C–C(=O)–O group	Acrylic medium
t1.23	1,105	Stretching vibration of ether –C–O–C– group	Polyethoxylated non-ionic surfactant
t1.24	1,060	Stretching vibration –C–O group	Polyethoxylated non-ionic surfactant
t1.25	1,020	Stretching vibration silicate	Burnt umber
t1.26	900–600	=C–H out-of-plane bending vibrations aromatic ring, C–H rocking vibration	Naphthol red, phthalo blue, burnt umber, zinc oxide

t2.1 **Table 2** The IR absorption bands of analytical interest identified in the studied Flashe® model paint film series before and after the 800-h simulated daylight exposure

t2.2	IR absorption band (cm^{-1})	Functional group assignment	Compound assignment
t2.3	3,400	–OH associated stretching vibration	Water of hydration
t2.4	2,961, 2,926	$–CH_3$ and $–CH_2$ antisymmetric stretching vibration	PVAc
t2.5	2,873	$–CH_3$ symmetric stretching vibrations	PVAc
t2.6	1,736	–C=O stretching vibration associated to acetate groups	PVAc
t2.7	$1,718^{s}$	–C=O stretching vibration associated to free acetic acid	PVAc
t2.8	1,410	Stretching vibration carbonate group	Calcium carbonate extender
t2.9	1,372	Bending vibration $–CH_2$ group	PVAc
t2.10	1,232	Asymmetric stretching mode of –C–(C=O)–C– of ester groups	PVAc
t2.11	1,113	Stretching vibration silicate group	Clayey material, burnt sienna
t2.12	1,086	Stretching vibration –C–O group	PVAc
t2.13	1,045	Stretching vibration	Polyethoxylated non-ionic surfactant
t2.14	900–600	=C–H out-of-plane bending vibrations aromatic ring	Senegal yellow
t2.15	871	Stretching vibration of carbonate group	Calcium carbonate extender
t2.16	712	Stretching vibration of carbonate group	Calcium carbonate extender

JmlID 216_ArtID 4294_Proof# 1 - 12/10/2010

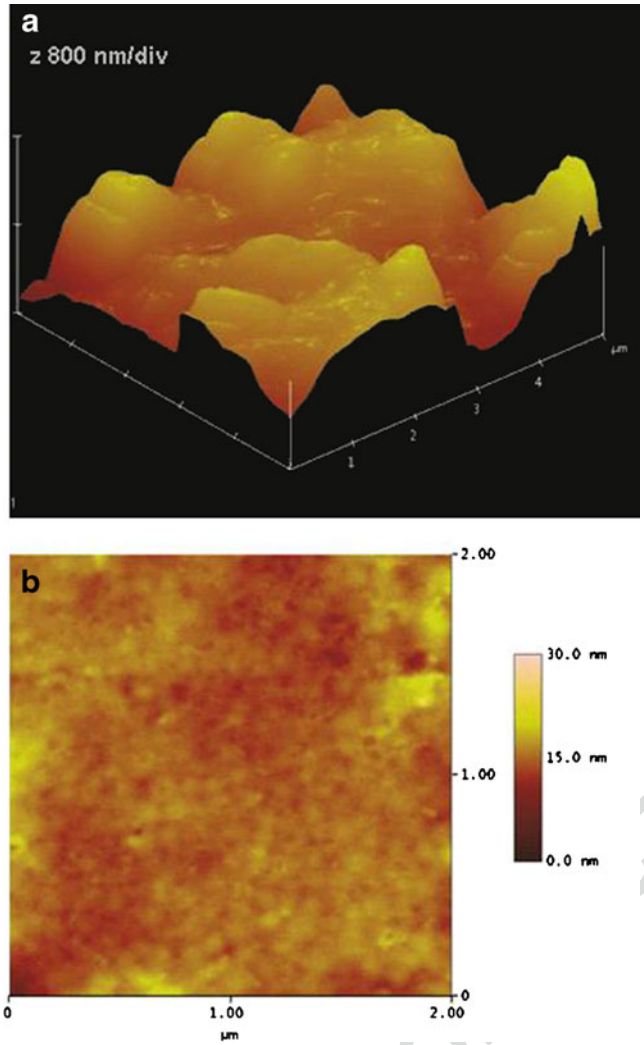

Fig. 6 Atomic force micrographs showing **a** air–film surface of the simulated-daylight-aged burnt umber Liquitex® paint film; **b** substrate–film surface of the unaged burnt umber Liquitex® paint film

A number of changes in the chemical composition of the model paint films series irradiated with an arc xenon lamp were also recognised by an FTIR spectroscopic analysis of the paint specimens' surfaces.

The Liquitex® paint film series exhibited a similar ageing behaviour irrespective of each colour's specific formulation. Thus, the IR spectra obtained in the Burnt umber (Fig. 8) paint film after the 400- and 800-h exposures to simulated daylight were dominated by the IR absorption bands corresponding to the PEO-type surfactant (2,884, 1,113 and 1,060 cm^{-1}). These results suggest that simulated daylight irradiation prompts the surfactant to migrate from within the film to its surface. Eventually, the intensity of the IR bands ascribed to the PEO-type surfactant reduced in some film surface areas after the 800-h exposure to simulated daylight. Such behaviour may be attributed to the oxidation of the long PEO molecules that cause the scission of the poly(oxyethylene) chains. The shorter chains formed are more compatible with the polymer, so they are able to diffuse back into the polymer [27, 28].

The IR band at 1,643 cm^{-1} in the IR spectra corresponds to the burnt umber and ZnO model paints irradiated with simulated daylight for 400 and 800 h. This band is ascribed to the bending vibrations of the –OH groups, which are associated with the water the hydration present in clayey materials that are included in the pigments and extenders used in these colours. This IR band appeared in parallel to a slight increase of the broad IR band at 3,400 cm^{-1}, which is ascribed to the stretching vibrations of the associated –OH groups. These changes suggest that simulated daylight irradiation may also prompt the free water molecules remaining in the interstices of the honeycomb structure of the completely non-coalesced paint films (Fig. 6b) to become fixed in these clayey minerals' structure.

Finally, the IR band at 1,563 cm^{-1} appearing in the IR spectra of the unaged zinc oxide and burnt umber paint films significantly dropped in the IR spectra of the 400- and 800-h aged films. This result suggests that these metal–surfactant complexes of the carboxylate type are extremely sensitive to simulated daylight irradiation.

The IR spectra obtained in the Flashe® model paint series irradiated with simulated daylight noticeably decreased in the weak sharp IR band at 1,045 cm^{-1}, which is ascribed to

Table 3 Shift of the L^*, a^*, b^* C^*, h^* and E* coordinates of the model paint films before and after the 800-h simulated daylight exposure

Model paint film	ΔL^*	Δa^*	Δb^*	ΔC^*	Δh^*	ΔE^*
PVAc: Flashe						
Oriental red	5.01	−10.39	−28.05	−25.73	−11.40	28.5
Green armour	15.16	22.38	−2.44	−22.44	2.97	15.4
Senegal yellow	0.76	2.13	−27.20	−26.94	−2.23	27.2
Burnt sienna	11.00	−13.59	−23.01	−25.78	11.92	25.5
Acrylic: Liquitex						
Zinc oxide	0.26	−0.13	1.30	1.13	−24.67	1.3
Burnt umber	16.76	−6.96	−9.40	−11.66	−4.97	19.2
Phthalo blue	18.87	−17.24	13.55	−20.06	−19.16	23.2
Naphthol red	7.10	−15.55	−28.37	−28.72	−13.02	29.2

Q1

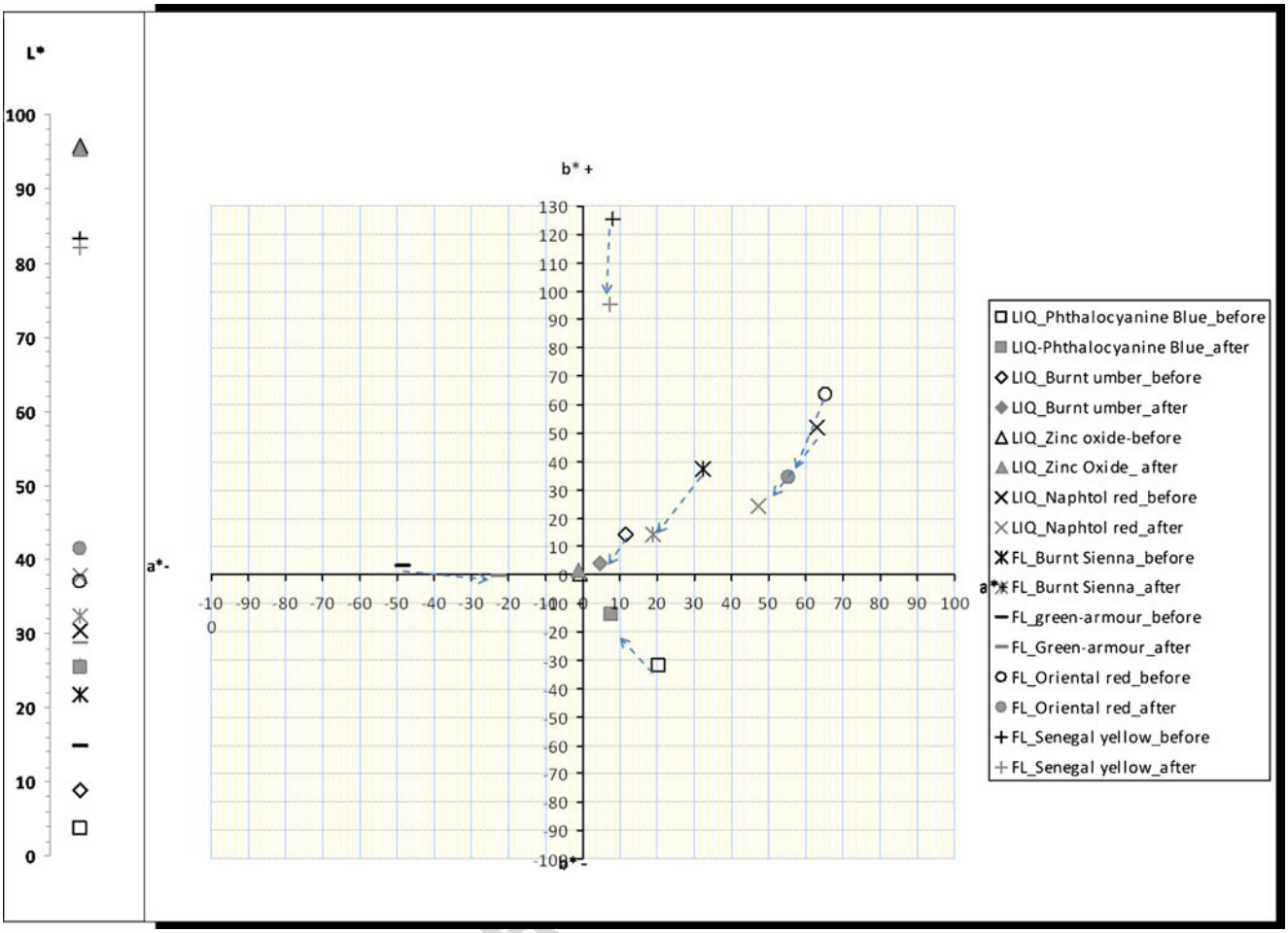

Fig. 7 L^* diagram and the a^* vs. b^* diagram that illustrates the changes in chrome and hue that the studied model paint films have undergone during simulated sunlight ageing

the PEO-type surfactant (Fig. 9), suggesting that a photodegradation process results in a significant loss of this stabiliser.

Regarding the polymer, recent literature proposes that a number of alteration processes, taking place in the PVAc polymer structure, may be recognised by comparing the IR spectra of the unaged and simulated daylight-aged paint films, for instance, chain scission due to ester cleavage or the fragmentation of polymer chains [12]. This process, which should take place during irradiation by a Norrish-Type II mechanism, results in the formation of acetic acid, which is accompanied by the formation of a double bond in the main chain. Accordingly, loss of intensity in the IR absorption bands ascribed to the polymer has been observed in the IR spectrum of aged paint films. In order to quantitatively evidence these changes, the integration of area (A) of the IR bands corresponding to the medium and calcium carbonate extender has been carried out. The results obtained in the studied Flashe® model paint films series are summarised in Table 4. Calcium carbonate was used as an internal standard because no structural changes by simulated daylight irradiation were expected. The A (ν C–O)/A (ν CO_3^{2-}) and A (ν C=O)/A (ν CO_3^{2-}) ratios corresponding to the stretching vibrations of the C–O and C=O groups present in the ester functionalities of the polymer chains have been used to assess the photodegradation that the polymer undergoes. The wavenumber intervals in the ranges of 1,279–1,210 cm^{-1} for ν (C–O), 1,760–1,725 cm^{-1} for ν (C=O) and 890–864 cm^{-1} for ν (CO_3^{2-}) have been used. The dependence of these values along with the simulated daylight irradiation time is also shown in Fig. 10a, b. In all cases, the medium/extender ratio value of the paint films irradiated for 400 h lowered. Afterwards, these values remained unchanged or only slightly changed after 800 h of simulated daylight irradiation. This result confirms that chain scission processes have taken place in the PVAc medium of the studied paint films within the first 400 h of irradiation, which is in good agreement with the results obtained with tensile strength tests (vide infra).

Broadening the ester IR bands as a result of the appearance of other carbonyl functions has also been observed in the studied paint film series. In particular, an

JnlID 216_ArtID 4294_Proof# 1 - 12/10/2010

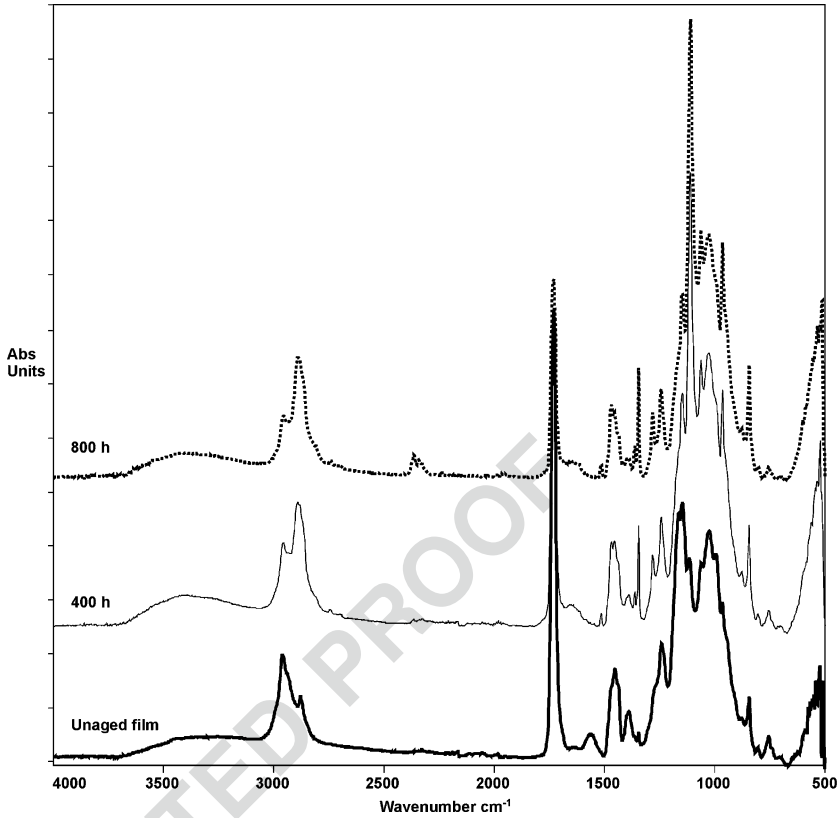

Fig. 8 The IR spectrum of the burnt umber Liquitex® paint film: **a** unaged paint film (*continuous line*); **b** 400-h simulated-daylight-aged paint film (*dotted line*); **c** 800-h simulated-daylight-aged paint film (*dashed line*)

increase in the shoulder at 1,718 cm^{-1} was associated with free acetic acid. This result is in good agreement with the loss of intensity of the IR bands ascribed to the PVAc medium. Integration of the IR bands corresponding to the stretching vibration of the C=O groups associated with both the ester groups (1,760–1,725 cm^{-1}) and the free acid groups (1,725–1,700 cm^{-1}) was also performed, and Table 4 provides the results obtained. Dependence of the integrated IR band area ratio values along with the irradiation time is illustrated in Fig. 10c. As Fig. 10c depicts, the content of free acid groups increased after 400 h of simulated daylight irradiation. In some cases, the IR band area ratio value slightly increased after an 800-h simulated daylight exposure.

A second alteration process affecting the PVAc polymer was the occurrence of side-chain reactions resulting in the loss of a CH_3 group in the polymer. This process taking place in the studied model paint film series was evidenced by comparing the $A(\nu\ CH_3)/A(\nu\ C{=}O)$ ratio values obtained by the integration of the IR bands area corresponding to both the stretching vibrations of the CH_3 group at 2,970–2,950 cm^{-1} and the stretching vibrations of the C=O group at 1,736–1,725 cm^{-1} (see Table 4). Figure 10d shows how this value for burnt Sienna remained unchanged but slightly decreased for the rest of the paints after 400 h of irradiation. The same trend was observed after 800 h of irradiation.

Surface hydrolysis of the acetate to poly(vinyl alcohol), also described by Bradford and Vanderhoff [28] as a frequent process taking place while drying PVAc films and further ageing, was not observed in the irradiated Flashe® paint films. In contrast, the characteristic stretching vibration IR band of the OH groups, which should evidence the presence of poly(vinyl alcohol), noticeably decreased in all the films under study after ageing. Absence of poly (vinyl alcohol) in the studied aged films could explain the loss of mechanical strength exhibited by the Flashe® films after simulated daylight ageing as this compound prevents the film from autohesion [28].

Finally, it should be noted that no information could be obtained from comparing the IR spectra of both the Liquitex® and Flashe® paint films in terms of polymer chain interdiffusion and the formation of entanglements among long polymer chains. This is a very interesting process as it has been considered to be mainly responsible for the film's gain in mechanical strength [31].

Mechanical properties

Unaged model paint films

Young's modulus values obtained for the unaged paint films of both the acrylic Liquitex® Heavy Body and PVAc Flashe® paints are listed in Table 5. The highest values are

Q1

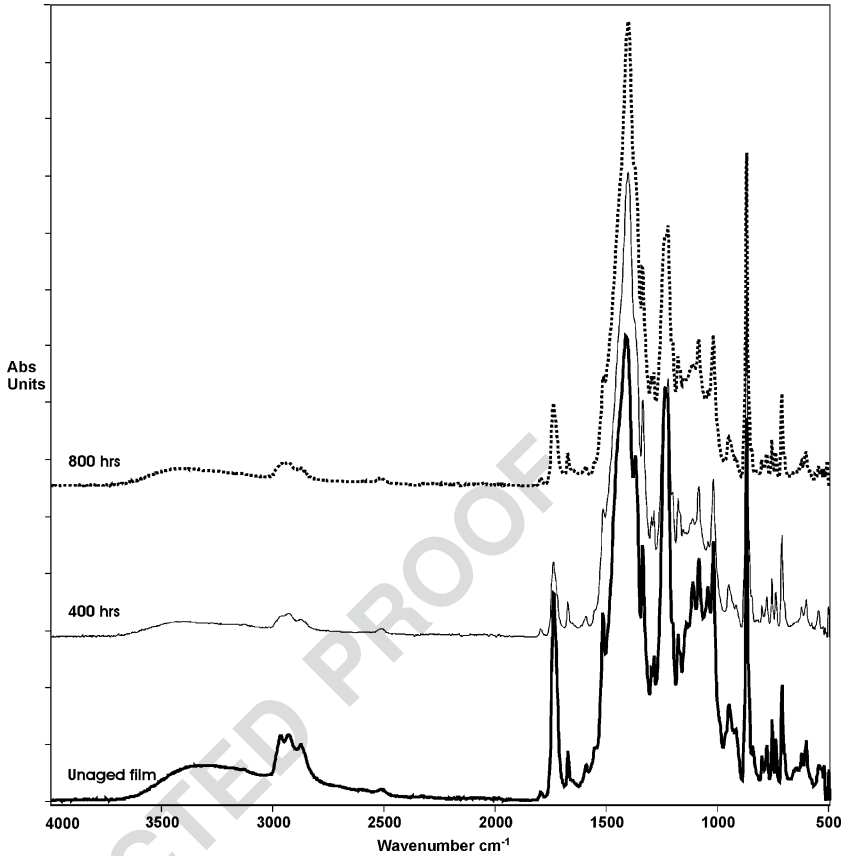

Fig. 9 The IR spectrum of the Senegal yellow Flashe® paint film: **a** unaged specimen (*continuous line*); **b** 400 h simulated-daylight-aged paint film (*dotted line*); **c** 800 h simulated-daylight-aged paint film (*dashed line*)

Q3

t4.1 **Table 4** Integrated IR band area ratios for the series of Flashe paints studied

t4.2 Model paint film	UV Light irradiation time (h)	Integrated IR band area (A) ratio			
t4.3		ν CH_3/ν C=O[a]	ν C=$O_{(acid)}$/ν C=O $_{(ester)}$[b]	ν C=O/ν CO_3^{2-}[c]	ν C–O/ν CO_3^{2-}[d]
t4.4 Senegal yellow	0	0.269±0.003	0.321±0.001	4.49±0.09	1.39±0.06
t4.5	400	0.240±0.004	0.362±0.004	3.14±0.09	0.56±0.04
t4.6	800	0.234±0.015	0.386±0.009	3.39±0.03	0.69±0.018
t4.7 Oriental red	0	0.24±0.02	0.32±0.04	3.9±0.5	1.2±0.11
t4.8	400	0.21±0.03	0.41±0.04	3.0±0.5	0.8±0.3
t4.9	800	0.21±0.02	0.41±0.04	2.8±0.3	0.58±0.08
t4.10 Burnt sienna	0	0.258±0.003	0.337±0.0015	3.62±0.04	1.14±0.05
t4.11	400	0.255±0.005	0.389±0.0017	3.20±0.03	0.67±0.03
t4.12	800	0.255±0.003	0.397±0.003	3.15±0.01	0.63±0.01
t4.13 Green armour	0	0.49±0.03	0.30±0.05	0.68±0.06	3.05±0.04
t4.14	400	0.41±0.04	0.37±0.08	0.23±0.02	1.97±0.13
t4.15	800	0.40±0.02	0.39±0.019	0.23±0.06	2.03±0.06

[a] Wavenumber intervals of integrated IR band area: ν CH_3 (2,970–2,950 cm^{-1}); ν C=O_{ester} (1,760–1,725 cm^{-1})

[b] Wavenumber intervals of integrated IR band area: ν C=O_{acid} (1,760–1,725 cm^{-1}); ν C=O_{ester} (1,725–1,700 cm^{-1})

[c] Wavenumber intervals of integrated IR band area: ν C–O (1,279–1,210 cm^{-1}); ν CO_3^{2-} (890–864 cm^{-1})

[d] Wavenumber intervals of integrated IR band area: ν C=O (1,760–1,700 cm^{-1}); ν CO_3^{2-} (890–864 cm^{-1})

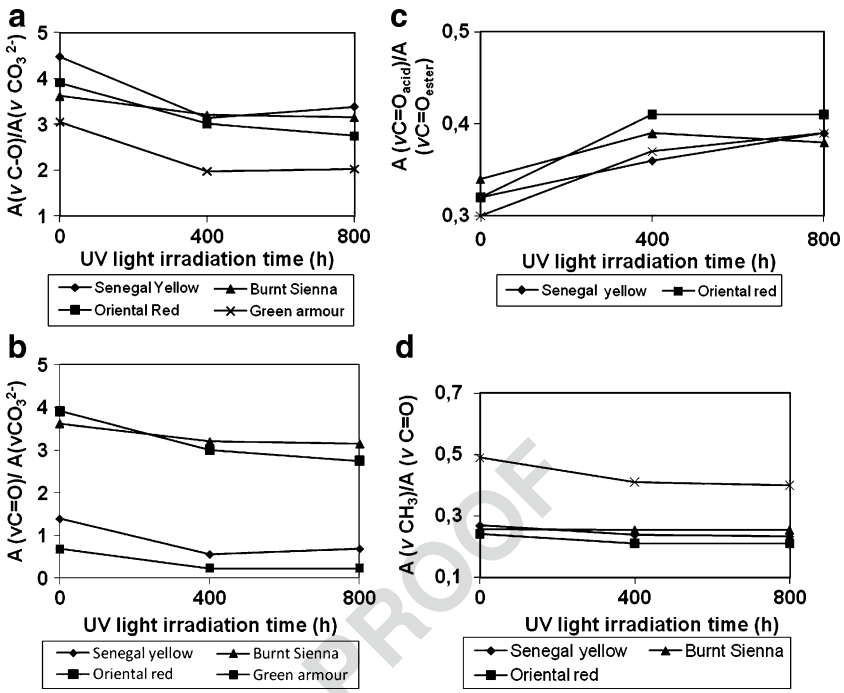

Fig. 10 The integrated IR band area ratio vs. simulated daylight irradiation time: **a** A (ν C–O)/A (ν CO_3^{2-}) ratio; **b** A (ν C=O)/A (ν CO_3^{2-}) ratio; **c** A (ν C=O_{acid})/A(ν C=O_{ester}); **d** A(ν CH_3)/A(ν C=O)

found in the PVAc paints in the following range: Burnt Sienna 30–Senegal yellow 33, compared with those from the acrylic Liquitex® series (Burnt umber 28–3). This result is in good agreement with the microscopic examination of specimens, which evidenced that the Flashe® model paints series has a higher pigment content.

Comparison of Young's modulus value of the Liquitex® paints prepared with organic pigments phthalo blue and naphthol red and with zinc oxide and burnt umber, these being pigments of an inorganic nature, indicates that noticeable differences in the mechanical behaviour of these model paints can be expected (see Table 5). These differences in mechanical properties may correlate with differences in the additive formulation associated with both pigment type and the degree of completion of the coalescence phase. The latter results in the formation of a continuous film from the interdiffusion of the polymer particles that come into contact with each other, thus rendering flexibility and cohesion properties. An AFM examination of the films showed that this process of further gradual coalescence was mostly delayed in those paints prepared with earth pigments, such as burnt umber.

Aged model paint films

In the general study frame of latex film formation and properties, the interdiffusion of polymer chains is described as the main process that provides the polymer film with mechanical strength. This process predominantly takes place in the last coalescence or annealing process steps that the film undergoes. Thus, increased strength is due to an initial interdiffusion step of the chain ends and the small

Table 5 Young's modulus values for the studied Liquitex® and Flashe® model paint film series

Colour	Young's modulus					
	Unaged paint film		400 h UV-light-aged		800 h UV-light-aged	
	E	*s*	*E*	*s*	*E*	*s*
Liquitex HB						
ZnO	21.2	0.2	16.7	0.7	15.1	0.4
Burnt umber	28	2	26	6	15.6	0.7
Phthalo blue	4.1	0.5	nd	nd	1.6	0.4
Naphthol red	3.07	0.11	2.4	0.5	2.5	0.3
Flashe						
Burnt sienna	30	3	51	7	61	3
Senegal yellow	33	4	61	3	48	4

E average value, *s* standard deviation, *nd* non-detected

JrnlID 216_ArtID 4294_Proof# 1 - 12/10/2010
Q1

chains in the still particulate film and then to the interdiffusion of longer chains accompanied by entanglements formation. While the film passes from a brittle fracture to a tough one during the former process, the latter process confers increasing toughness to the film.

Photodegradation of the polymer film can result in the occurrence of the cross-linking of chains leading to films of reduced strength if the distance among the cross-linked chains is shorter than the entanglement length [29].

The pigment effect has to be also considered in a complete study of paint films' mechanical properties. High pigment content results in significantly increased stiffness. In particular, increased brittleness and hardness have been previously reported as the overall physical effects of light on acrylic paints [32].

In this context, measuring the mechanical properties of the model paint films series prepared in this work can be of great assistance in determining the effects of light exposure on paint films. Comparison of the stress curves versus the strain curves obtained for unaged and simulated daylight-aged model paint films enables the characterisation of the mechanical behaviour of materials when they are subjected to an intense source of simulated daylight.

In this study, Young's modulus value obtained in the paint film specimens irradiated with simulated daylight for 400 and 800 h notably decreased for the Liquitex® Heavy Body colours, as shown in Table 5. In parallel, the elongation-at-break values slightly increased, as illustrated in Fig. 11, which depicts the stress–strain curves obtained for the naphthol red colour. A lower Young's modulus value after ageing corresponds to a lessening of the paints' stiffness. This result is coherent with the morphological and structural changes noted by the microscopy and spectroscopy techniques. Thus, further gradual coalescence results in a well-formed polymeric film, which is prompted by simulated daylight irradiation. These processes confer paint films a more regular surface and improved elasticity if compared with unaged films. Exudation of surfactants, their probable photodegradation and further diffusion back into the polymer do not seem to be significant influence factors on the mechanical properties of paint films.

An increased Young's modulus value was, in contrast, found for the Flashe® series, as Table 5 and Fig. 12 show. Greater stiffness and, in general, decay of the mechanical properties of the studied Flashe® paint films are coherent with the higher pigment content and the various photodegradation processes identified by FTIR spectroscopy, particularly chain scission, consisting of ester cleavage or the fragmentation of polymer chains as well as side-chain reactions. Photodegradation of surfactants, which is another process identified by FTIR spectroscopy, could also contribute to the changes observed in the mechanical properties, be it to a lesser extent.

Conclusions

Examination by LM, SEM/EDX, AFM, UV-vis spectrophotometry and FTIR spectroscopy and performing tensile tests all provide complementary information on the overall

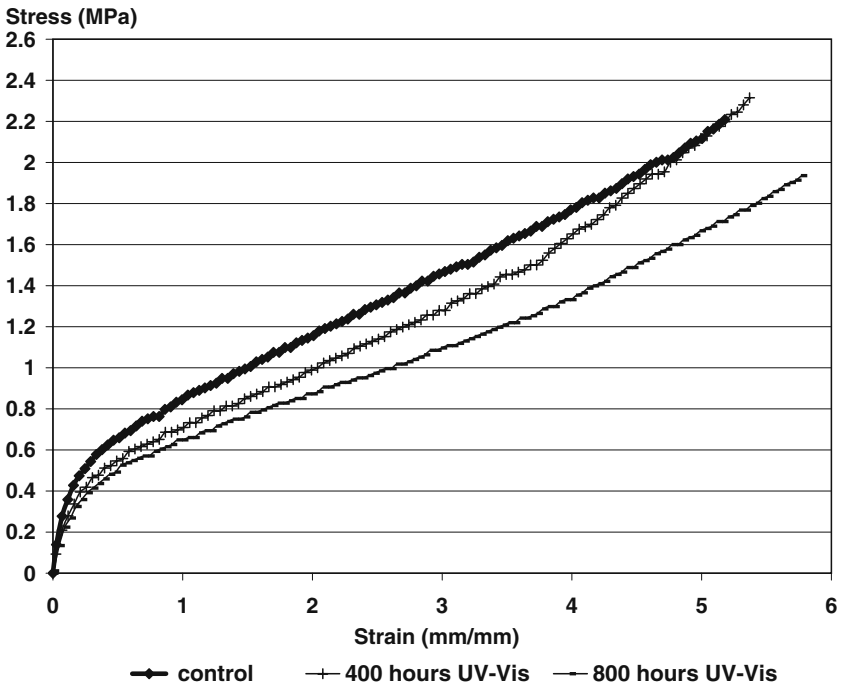

Fig. 11 The stress vs. the strain curves for the unaged and the 400- and 800-h simulated-daylight-aged naphthol red Liquitex® HB

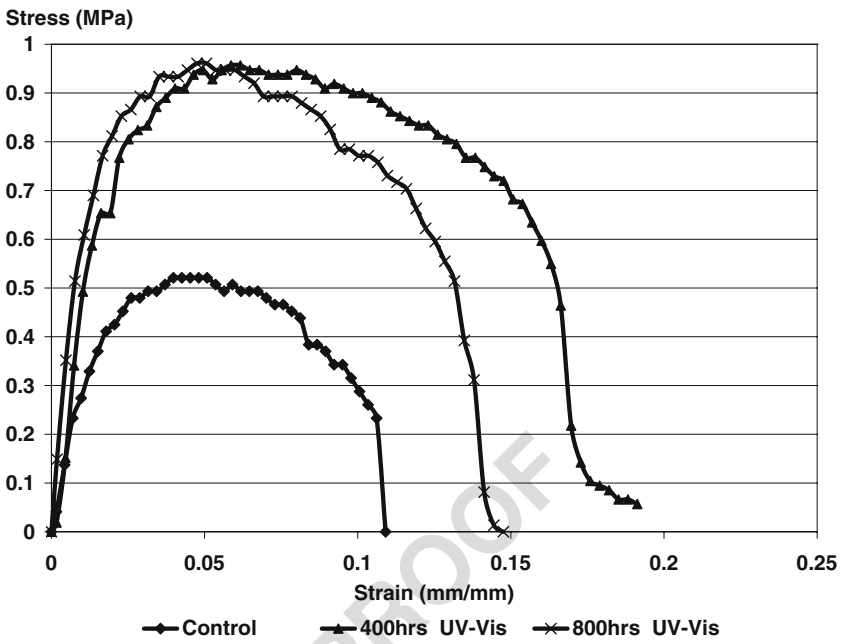

Fig. 12 The stress vs. the strain curves for the unaged and the 400- and 800-h simulated daylight-aged burnt sienna Flashe®

behaviour of the studied paint films. Changes in morphology, composition and the mechanical properties correlate, while the results evidence differences in the ageing behaviour of the acrylic and PVAc series of colours studied. Additionally, different behaviours of the colours in the Liquitex® series are noted in accordance with the pigment and, consequently, the additive formulation used by the manufacturer.

As expected, simulated daylight exposure results in noticeable changes in the visual appearance of the model paints series tested. It is interesting to note that the results obtained suggest that the changes in the studied paints depend on the type of pigment and on the binding medium. In general, the studied paints' chrome and hue negatively shift, and their variation takes place at a greater or lesser extent, depending on each pigment's fading tendency or light sensitivity, whereas changes in lightness (L^*) are more associated with the behaviour of the binding medium during the ageing treatment. Thus, those paints containing pigments of an inorganic nature exhibit the lowest ΔC^* values. Comparison between those paints containing organic pigments evidences that those prepared with pigments from the phthalocyanine group display a slightly better behaviour than the rest of the paints containing organic pigments.

The results obtained by combining microscopy and spectroscopic techniques suggest that the formulation of paints influences the film formation process and, therefore, the film's final structure, composition and mechanical properties. Thus, Liquitex® heavy body, in which the relative amount of surfactant probably increases to stabilise the pigment in the paint emulsion, exhibits notable PEO surface migration and an altered film surface morphology. Specific surfactants of an anionic type have also been identified in those Liquitex® colours containing inorganic pigments. In contrast to the acrylic brand, Flashe® PVAc colours have a high pigment content that results in the film's enhanced stiffness.

Simulated daylight irradiation has different effects on the two acrylic and PVAc brands under study. The migration of surfactants from the bulk to the film surface as well as film formation completion, particularly in those films containing an inorganic pigment, determines a lessening of the Liquitex® acrylic film' stiffness. Photodegradation of both the surfactant and polymer, the latter including chain scission and side-chain processes, has resulted in increased stiffness of the simulated daylight-irradiated Flashe® PVAc colours.

In view of these results, the different behaviours of acrylics and PVAc emulsion paints should be considered for preventive conservation purposes, since they show very different responses to light exposure.

In practice, PVAc type of paints requires special attention when exposed to light since they are prone to suffer degradation of the polymeric chains beyond degradation of the surfactant additives. As a consequence, there is a substantial change in the mechanical strength of these paints. On the other hand, the acrylic films have shown higher stability during the ageing tests performed.

For both types of paints, it is evident that the curing of their respective binding media is a complex process that depends on pigments and additives, and it takes much more time than the simple drying of water from the initial emulsion system. This is a relevant finding when facing cleaning issues in aged acrylic and PVAc emulsion paints.

Q1

It may be interesting to consider the surfactant deposed in the surface as an intrinsic protective layer which is prone to vanish with time. Rather than curative conservation (cleaning treatments), special effort should be spent in preventive conservation (good ventilation to avoid dirt depositing, safe handling, etc.).

Acknowledgements Financial support is gratefully acknowledged from the Spanish "I+D+I MICINN" project CTQ2008-06727-C03-01/BQU supported by ERDEF funds and from the "Generalitat Valenciana" I+D project ACOMP/2009/171 and the AP2006-3223 project ascribed to the Predoctoral Stages Programme of Universitary Researchers in Spanish Universities and Research Centres from the Spanish Ministry of Science and Innovation (MICINN). The authors wish to thank Mr. Manuel Planes i Insausti and Dr. José Luis Moya López, the technical supervisors responsible for the Electron Microscopy Service at the Polytechnic University of Valencia.

Q4

References

1. Learner TJS (2004) Analysis of modern paints. Getty Conservation Institute, Los Angeles, and references therein
2. Ormsby B, Learner T (2009) Rev Conserv 10:29–42
3. Silva MF, Doménech-Carbó MT, Fuster-López L, Mecklenburg MF, Martin-Rey S (2010) Anal Bioanal Chem 397:357–367
4. Hoogland FG, Boon JJ (2009) Int J Mass Spectrom 284:72–80
5. Hoogland FG, Boon JJ (2009) Int J Mass Spectrom 284:66–71
6. Learner T, Chiantore O, Scalarone D (2002) In: Preprints ICOM Committee for Conservation 13th Triennial Meeting. James & James, London, pp 911–919
7. Whitmore PM, Colaluca VG (1995) Stud Conserv 40:51–64
8. Chiantore O, Trossarelli L, Lazzari M (2000) Polymer 41:1657–1668
9. Chiantore O, Lazzari M (2001) Polymer 42:17–27
10. Scalarone D, Chiantore O, Learner T (2005) In: Preprints ICOM Committee for Conservation 14th Triennial Meeting. James & James/Earthscan, London, pp 350–358
11. Melo MJ, Bracci S, Camaiti M, Chiantore O, Piacenti F (1999) Polym Degrad Stab 66:23–30
12. Ferreira JL, Melo MJ, Ramos AM (2010) Polym Degrad Stab 95:453–461
13. Schultz AR (1961) J Phys Chem 65:967–972
14. Allara DL (1975) Environ Health Perspect 11:29–33
15. Ferreira JL, Melo MJ, Ramos AM (2010) Polym Degrad Stab 95:453–461
16. Whitmore PM, Colaluca VG, Farrell E (1996) Stud Conserv 41:250–255
17. Digney-Peer S, Burnstock A, Learner T, Khanjian H, Hoogland F, Boon J (2004) In: Roy A, Smith P (eds) Modern art. International Institute for Conservation of Historic and Artistic Works, London, pp 202–207
18. Ormsby B, Hoogland F, Smithen P, Miliani C, Learner T (2008) In: Proceedings of the 15th Triennial Meeting of the ICOM Committee for Conservation. James & James, London, pp 857–865
19. Doménech-Carbó MT, Bitossi G, Osete-Cortina L, de la Cruz-Cañizares J, Yusá-Marco DJ (2008) Anal Bioanal Chem 391:1371–1379
20. Feller RL (1978) In: Proceedings of the 5th Trienial Meeting ICOM Committee for Conservation, James & James, London, 78/16/4/1-11
21. Bunsen RW, Roscoe HE (1859) Philos Trans R Soc Lond 149:879–926
22. Schwarzschild K (1990) Astrophys J 11:89–91
23. Amalvy JI, Soria DB (1996) Prog Org Coat 28:279–283
24. Horgnies M, Darque-Ceretti E, Combarieu R (2003) Prog Org Coat 47:154–163
25. Hellgren ACh, Weissenborn P, Holmberg K (1999) Prog Org Coat 35:79–87
26. Chiantore O (2002) In: Mattison G (ed) The Fifth Annual Infrared and Raman Users Group Conference. The Getty Conservation Institute, Los Angeles, pp 92–95
27. Bradford EB, Vanderhoff JW (1966) J Macromol Chem 1:335–360
28. Bradford EB, Vanderhoff JW (1972) J Macromol Sci Phys B6:671–694
29. Steward PA, Hearn J, Wilkinson MC (2000) Adv Colloid Interface Sci 86:195–267
30. Doménech-Carbó MT, Silva MF, Aura-Castro E, Doménech-Carbó A, Fuster-López L, Gimeno-Adelantado JV, Kröner SU, Martínez-Bazán ML, Más-Barberá X, Mecklenburg MF, Osete-Cortina L, Yusá-Marco DJ (2010) In: Fuster L, Doménech MT, Mecklenburg MF, Charola H (eds) Preprints of cleaning 2010—new insights into the cleaning of paintings. Universidad Politécnica de Valencia, Valencia, pp 39–40
31. Zosel A, Ley G (1992) Polym Bull 27:459–464
32. Zosel A, Ley G (1993) Macromolecules 26:2222–2227
33. Jablonski E, Learner T, Hayes J, Golden Mark (2003) Rev Conserv 1–13